BBA - Bioenergetics 1860 (2019) 651–658

Contents lists available at ScienceDirect

BBA - Bioenergetics

journal homepage: www.elsevier.com/locate/bbabio

Digitonin-sensitive LHCII enlarges the antenna of Photosystem I in stroma lamellae of *Arabidopsis thaliana* after far-red and blue-light treatment

Peter Bos[a], Anniek Oosterwijk[a], Rob Koehorst[a,b], Arjen Bader[a,b], John Philippi[a], Herbert van Amerongen[a,b], Emilie Wientjes[a,*]

[a] Laboratory of Biophysics, Wageningen University, P.O. Box 8128, 6700 ET Wageningen, the Netherlands
[b] MicroSpectroscopy Research Facility, Wageningen University, P.O. Box 8128, 6700 ET Wageningen, the Netherlands

ARTICLE INFO

Keywords:
Light-harvesting complex
State transition
Excitation-energy transfer
Time-resolved fluorescence
Photosystem

ABSTRACT

Light drives photosynthesis. In plants it is absorbed by light-harvesting antenna complexes associated with Photosystem I (PSI) and photosystem II (PSII). As PSI and PSII work in series, it is important that the excitation pressure on the two photosystems is balanced. When plants are exposed to illumination that overexcites PSII, a special pool of the major light-harvesting complex LHCII is phosphorylated and moves from PSII to PSI (state 2). If instead PSI is over-excited the LHCII complex is dephosphorylated and moves back to PSII (state 1). Recent findings have suggested that LHCII might also transfer energy to PSI in state 1. In this work we used a combination of biochemistry and (time-resolved) fluorescence spectroscopy to investigate the PSI antenna size in state 1 and state 2 for *Arabidopsis thaliana*. Our data shows that 0.7 ± 0.1 unphosphorylated LHCII trimers per PSI are present in the stroma lamellae of state-1 plants. Upon transition to state 2 the antenna size of PSI in the stroma membrane increases with phosphorylated LHCIIs to a total of 1.2 ± 0.1 LHCII trimers per PSI. Both phosphorylated and unphosphorylated LHCII function as highly efficient PSI antenna.

1. Introduction

Light energy absorbed by photosystem I (PSI) and photosystem II (PSII) drives photosynthesis. Along the linear electron transport chain the photosystems work in series to extract electrons from water and reduce $NADP^+$ to NADPH [1]. As a consequence light energy can be used most efficiently when the excitation pressure on the two photosystems is balanced. However, the light spectrum can change during the day: For instance, a plant located under a tree may be directly illuminated in the morning when the sun is close to the horizon, whereas it only receives canopy shade light at midday. Canopy shade light is enriched in far-red light, which drives PSI far stronger than PSII [2]. If PSI is over-excited the plastoquinone pool gets oxidized; instead the plastoquinone pool becomes reduced when PSII is over-excited. State transitions constitute the process which rebalances the excitation pressure by redistributing the major light-harvesting complex (LHCII) between PSI and PSII [3,4]. If the plastoquinone pool is reduced Stn7 kinase gets activated and phosphorylates LHCII [5]. A special pool of LHCII complexes, called “extra” LHCII [6], is mobile and dissociates from PSII and associates with PSI upon phosphorylation (state 2). When the plastoquinone pool is oxidized the Stn7 kinase is deactivated and TAP38/PPH1 phosphatase dephosphorylates LHCII, which then moves back to PSII (state 1) [7,8].

In the past few years it has been shown that the mobile LHCII trimer is composed of $Lhcb1_2Lhcb2_1$ subunits, and that phosphorylation of Lhcb2 is required for its association with PSI [9–11]. Indeed, the recently published crystal structure of the PSI-LHCII supercomplex shows that the phosphorylated threonine of Lhcb2 strongly interacts with the PsaL subunit of the PSI core and that the N-terminus of Lhcb2 interacts with the PsaH, PsaL and PsaO subunits [12]. The involvement of these subunits is in agreement with the strong reduction of state transitions in plants deprived of these proteins [13,14].

In state-2 conditions at most ~50% of PSI is found in a digitonin stable PSI-LHCII supercomplex, where the antenna cross section of PSI is enlarged by one phosphorylated LHCII (LHCII-P) trimer associated at the PsaH/L/O side of the PSI core [7,13,15–19]. However, an increasing amount of data shows that additional LHCII trimers can associate with PSI: 1) In a detergent-free membrane preparation from spinach multiple LHCII trimers were energetically connected to PSI [20,21]. 2) Even in the absence of phosphorylation LHCII works as an antenna of PSI [16,22]. 3) In mutants lacking the Lhca light-harvesting complexes of PSI the extent of state transitions is reduced, indicating a

* Corresponding author.
E-mail address: emilie.wientjes@wur.nl (E. Wientjes).

https://doi.org/10.1016/j.bbabio.2019.07.001
Received 23 November 2018; Received in revised form 14 June 2019; Accepted 7 July 2019
Available online 09 July 2019

role for these proteins in the association of LHCII [22]. 4) PSI-LHCII$_2$ particles with one LHCII trimer at the PsaH and one LHCII trimer close to Lhca2 were observed with electron microscopy [23]. 5) An LHCII trimer to PSI ratio of ~0.8 was found for stroma membranes isolated from state-1 plants which are devoid of the digitonin stable PSI-LHCII supercomplexes [24].

Thus far it is not clear to which extent the antenna size of PSI is enlarged by LHCII under state-1 and state-2 conditions. In this work we use ultrafast time-resolved fluorescence to investigate how much the PSI antenna is enlarged by LHCII in intact leaves and isolated stroma lamellae in state 1 and state 2. The data shows that digitonin-sensitive LHCII transfers energy to PSI with high efficiency.

2. Materials and methods

2.1. Plant material

Arabidopsis thaliana (Col) wild type and ΔStn7 mutant (SALK_073254) were grown at 80 , 22 °C and 12 h of daylight. Plants of 6 to 8 weeks old were used for the experiments.

2.2. Thylakoid isolation

Plants were illuminated with blue LED light (max. at 467 nm, FWHM 26 nm) or far-red LED light (max. at 707 nm, FWHM 22 nm) for 45 min to induce state-2 or state-1, respectively. The light intensity was 10 ± 5 μmol photons/m^2/s. Thylakoid isolation was performed as described earlier [25], but with a few modifications in the buffer composition. Buffer 1 was composed of 0.4 M sorbitol, 5 mM $MgCl_2$, 20 mM tricine, 5 mM EDTA and 10 mM $NaHCO_3$, buffer 2 of 0.3 M sorbitol, 5 mM $MgCl_2$, 20 mM tricine, 2.5 mM EDTA and 10 mM $NaHCO_3$ and buffer 3 of 5 mM $MgCl_2$, 2.5 mM EDTA and 20 mM Hepes. To all buffers 10 mM NaF was added to inhibit phosphatase activity.

2.3. Stroma lamellae isolation

Stroma lamellae were isolated according to [26]. In short, freshly prepared thylakoids were mildly solubilised with digitonin at a final concentration of 1.0% with a chlorophyll concentration of 0.3 mg/ml. The grana were pelleted by centrifugation at 40,000*g* for 30 min, and the stroma lamellae were separated by centrifugation at 140,000*g* for 90 min.

2.4. Pigment analysis and PAGE

The absorption spectra of pigments extracted in 80% acetone were recorded from 350 nm to 750 nm and fitted with the spectra of the individual pigments to obtain the chlorophyll *a/b* ratio, as described in [27]. Blue-native PAGE was performed according to [17]. The final concentration of digitonin was 1% at a chlorophyll concentration of 0.5 mg/ml. Modified Laemmli SDS-PAGE was performed according to [28]. Phosphorylated proteins were stained with Pro-Q® Diamond Phosphoprotein Gel Stain (ProQ) and visualised with an Ettan DIGE imager from GE healthcare after excitation at 540 nm. Subsequently, the gel was stained with 0.05% Coomassie R in 40% methanol and 10% acetic acid and imaged with a Universal Hood II from BioRad.

2.5. Stroma lamellae solubilisation and 77 K fluorescence

Stroma membranes at a chlorophyll concentration of 0.25 mg/ml were solubilised with an equal volume of 1% α-dodecylmaltoside (α-DM) and left for 10 min on ice. To stop the solubilisation 10 parts of 50% glycerol, 5 mM tricine pH 7.8 were added for the 77 K steady-state fluorescence and 10 parts of buffer 1 for the samples for the streak-camera measurements. The 77 K fluorescence spectra were recorded on a Fluorolog 3.22 spectrofluorimeter (HORIBA Jobin Yvon, Longjumeau, France), after excitation with 470 nm light. The measurements were performed on samples in a glass Pasteur pipette (path length ~1 mm) which was placed in a liquid nitrogen containing glass dewar.

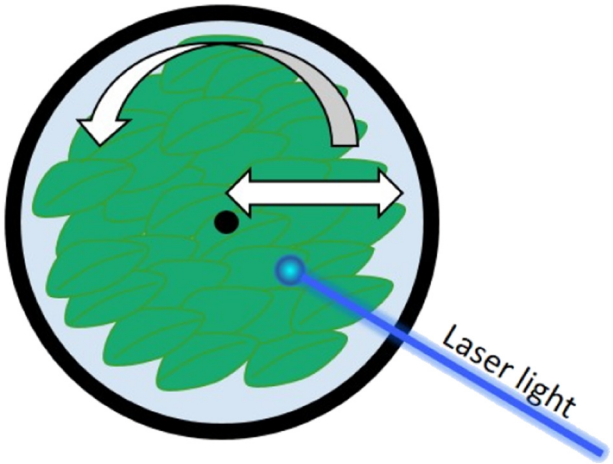

Fig. 1. Rotating and translating leaf cuvette. For the time-resolved experiments leaves were placed in a cuvette which rotates and moves sideways as indicated in the figure. The laser light hits the leave circa 1 cm below the center.

2.6. Streak-camera measurements

Time-resolved fluorescence measurements were performed with a streak-camera system as described previously [29]. Intact *A. thaliana* leaves were placed in a circular cuvette that simultaneously rotates and moves sideways as shown in Fig. 1 and explained in [30,31]. To excite the leaves pulsed laser light with a repetition rate of 3.8 MHz, a wavelength of 400 nm or 483 nm and an intensity of 30 μW, was focussed on the leaves in a spot with a diameter of ~100 μm. A power study showed that this laser intensity in combination with a rotation speed of 1 rpm and a sideways movement of 2 rpm was high enough to close the PSII reaction centers and low enough to avoid singlet–singlet annihilation. Prior to the measurements leaves where illuminated for at least 15 min with 15 μmol photons/m^2/s of far-red 707 nm LED light to induce state-1, or with 10 μmol photons/m^2/s of blue 467 nm LED light to induce state-2. The LED light remained on during the measurements of ~6 min. Stroma lamellae were measured in a 1 cm × 1 cm cuvette at a chlorophyll concentration of 20 μg/ml. The sample was continuously stirred during the measurement. The time-window for all measurements was 2 ns.

2.7. Data analysis time-resolved fluorescence

The collected streak images were corrected for background signal and for spatial variation of detection sensitivity. The corrected datasets were globally analysed using Glotaran and described with decay-associated spectra [32,33]. The spectra measured on leaves were corrected for reabsorption of the fluorescence by dividing the signal by the transmission spectra of isolated thylakoids measured with an integrating sphere. The transmission was normalized such that the emission of the PSII spectrum at its maximum at ~680 nm was 5 times as strong compared to the vibrational tail at 720 nm [34,35]. The transmission ranged between 0.7 and 1.0 for all measurements. All decay associated spectra were normalized to have the same area under the sum of the spectra. In the leaves two nanosecond lifetimes of 1 ns and 3 ns were resolved, associated with the same spectral shape of PSII, e.g. [34]. The sum of both spectra is shown in Fig. 2 together with the average lifetime calculated as: $< \tau > = \Sigma A_i * \tau_i$, with A_i the relative area under the spectrum i and τ_i the corresponding lifetime.

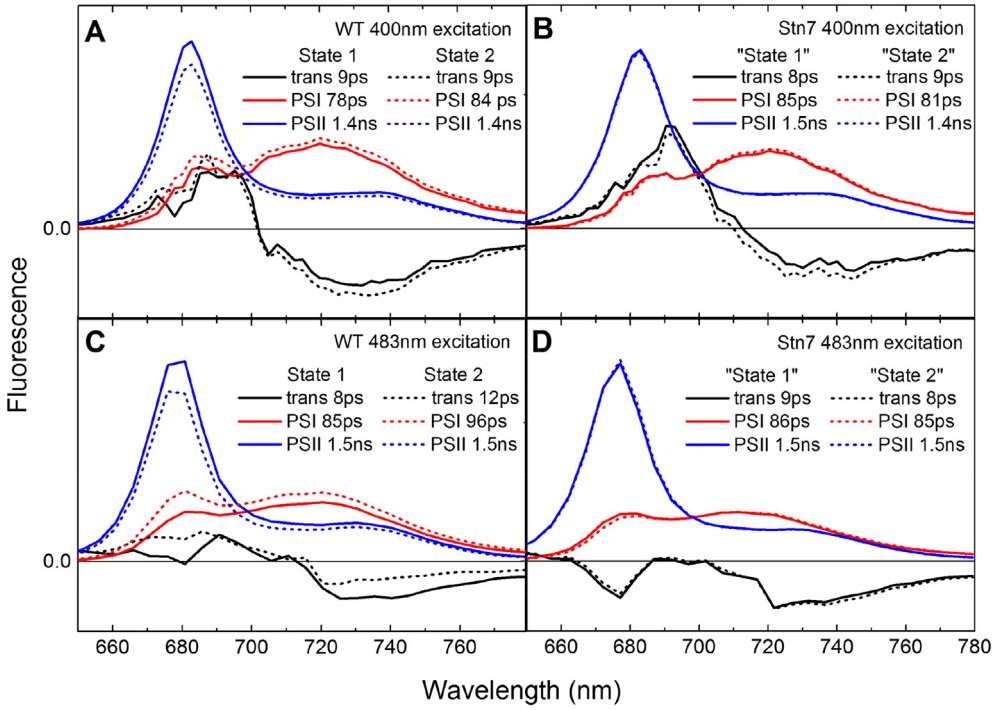

Fig. 2. Fluorescence decay of *A. thaliana* leaves. Decay-associated spectra of wild-type and ΔStn7 leaves after 400 nm and 483 nm excitation. The leaves were illuminated with far-red light (state-1) or blue light (state-2) before and during the measurement.

2.8. Calculation of the change in PSI antenna size upon state transitions

The decay-associated spectra of intact leaves show that upon 400 nm excitation the change in PSI antenna size qT_{PSI}, defined as $(F_{PSI\text{-}State\text{-}2} - F_{PSI\text{-}State\text{-}1}) / F_{PSI\text{-}State\text{-}2}$, is 0.11 ± 0.01 (based on 2 independent biological replicates). The change in fluorescence of PSI is directly related to the change in the absorption cross section of PSI. If the absorption of PSI in state 1 at 400 nm is known, then the absorption can be calculated for state-2. According to the analysis of the stroma membranes the PSI antenna size is enlarged by 0.7 LHCII trimers in state 1. The absorption spectra normalized to the number of chlorophylls (Fig. 6) show that at 400 nm the absorption of PSI is $Abs_{PSI\ 400nm} = 1.664$ (arbitrary units) and that of LHCII is $Abs_{LHCII\ 400nm} = 0.417$ a.u.. As such the PSI absorption is 1.664 + 0.7*0.417 = 1.955 a.u. in state-1. The difference in absorption between state 2 and state 1 is given by the number of LHCII trimers (n) that associate with PSI upon transition to state-2 and the LHCII absorption at 400 nm ($Abs_{LHCII\ 400nm}$). Hence, $qT_{PSI} = n*0.417 / (1.955 + n*0.417) = 0.11 \pm 0.01$. It follows that $n = 0.58 \pm 0.06$. The calculations are the same for 483 nm excitation, with $Abs_{PSI\ 483nm} = 0.931$ and $Abs_{LHCII\ 483\ nm} = 0.572$.

3. Results

3.1. Quantifying state transitions with time-resolved fluorescence

The conventional method to measure state transitions is pulse amplitude modulated (PAM) fluorescence. With this method the relative antenna size of PSII is estimated from the fluorescence level during a saturating light pulse which closes the PSII reaction centers. The fluorescence quantum yield of PSI is low [21,36–40] and virtually independent of the open/closed state of the reaction center [41]. As such, the contribution of this photosystem to the total fluorescence is small and usually neglected. Another way to quantify state transitions is time-resolved fluorescence with a streak camera. The advantages of this method are that both temporal and spectral information is acquired and that changes in the antenna size can be quantified for both photosystems.

Wild-type and ΔStn7 *A. thaliana* leaves, which lack the LHCII kinase, were placed in a rotating and translating circular cuvette (see Materials and Methods for details). The movement of the cuvette in combination with the intensity of the laser light was chosen such that the PSII reaction centers were closed by the laser light. In this condition the fluorescence of PSII decays on the ns timescale, while the fluorescence of PSI decays in < 100 ps. Leaves were illuminated with 15 µmol photons/m^2/s far-red light to induce state 1 or with 10 µmol photons/m^2/s blue light to induce state 2. Two laser excitation wavelengths were used, 400 nm and 483 nm. At 483 nm LHCII, which is rich in chlorophyll *b*, is preferentially excited, while 400 nm is rather unselective for either PSI, PSII or LHCII. The wavelength-dependent fluorescence decay was described by decay associated spectra (Fig. 2). After 400 nm excitation the shortest lifetime of ~10 ps is associated with a spectrum with a positive maximum around 680 nm and a negative maximum around 730 nm. This reflects transfer of excitation energy from chlorophylls emitting at 680 nm to red-shifted chlorophylls emitting around 720 nm, typical for PSI [42]. The second spectrum is associated with a lifetime of 80–90 ps and shows a maximum around 720 nm, which reflects excitation-energy trapping by PSI [21,36–40]. The last spectrum has an average lifetime of 1.4 ns and represents the fluorescence decay of PSII with closed reaction centers [30,34]. In wild-type leaves the antenna size of PSII decreases in state-2, as compared to state-1, while the opposite change occurs in PSI. The level of state transition can be quantified based on the fluorescence drop of PSII, called qT [43]. The total PSII emission is given by the area under the PSII spectrum, thus $qT_{PSII} = (F_{PSII\text{-}State\text{-}1} - F_{PSII\text{-}State\text{-}2}) / F_{PSII\text{-}State\text{-}1}$. And in analogy we can also quantify the relative change in antenna size of PSI, $qT_{PSI} = (F_{PSI\text{-}State\text{-}2} - F_{PSI\text{-}State\text{-}1}) / F_{PSI\text{-}State\text{-}2}$. After 400 nm excitation qT_{PSI} is 0.11 ± 0.01 and qT_{PSII} is 0.12 ± 0.01. The qT_{PSII} value is in good agreement with the results based on PAM measurements (see e.g. [6,22]). Furthermore, a similar change in the antenna size of PSI and PSII during state transitions is in agreement with a relative antenna size ratio of PSI vs PSII of ~1 [34,44]. For ΔStn7 leaves, the qT parameters after 400 nm and 483 nm excitation were both close to zero (≤0.01) as anticipated in absence of the LHCII kinase [5]. The stronger excitation

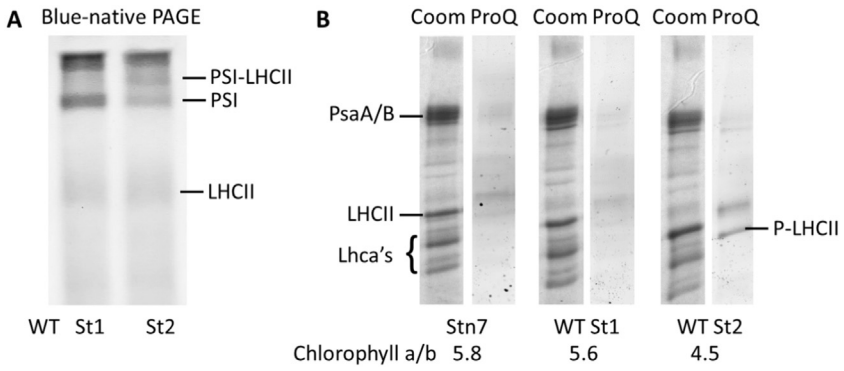

Fig. 3. Protein composition and phosphorylation level. A. Thylakoid membranes (8 μg of chlorophylls) were solubilised with 1% digitonin and subjected to blue-native PAGE separation. The location of the PSI-LHCII, PSI and LHCII complexes according to [17,19] is indicated. B. SDS-PAGE gel with stroma lamellae isolated from Stn7, state-1 wild-type (St1 WT) and state-2 wild-type (St2 WT) leaves. The proteins are stained with Coomassie Blue (Coom), and the phosphorylated proteins with ProQ diamond (ProQ). The position of the PSI core proteins PSA/B, the PSI Lhca's and LHCII is indicated. A small amount of PSII proteins is present in all three stroma membranes as can be judged from the faint bands in between PsaA/B and LHCII. In Stn7 and state-1 stroma membranes LHCII is present which is virtually unphosphorylated, while phosphorylated LHCII (P-LHCII) is found in state-2 membranes. The chlorophyll *a*/b ratio is based on 2 measurements, the standard deviation was < 0.03 for all samples.

of LHCII at 483 nm is expected to result in larger changes of the PSI and PSII antenna absorption upon state transitions. This is indeed observed for wild-type leaves (Fig. 2C). The qT value for PSII is 0.14 ± 0.01 and qT_{PSI} is even 0.19 ± 0.01. The 80–90 ps state-2 spectrum of PSI shows the strongest increase at 680 nm relative to state-1, which can be ascribed to the emission of LHCII which has its fluorescence maximum at this wavelength [21,45].

3.2. Digitonin sensitive LHCII is present in stroma lamellae of state-1 and state-2 plants

The thylakoid membranes of plants illuminated with far-red or blue light were isolated. The membranes were digitonin solubilised and run on a blue-native PAGE gel (Fig. 3A). After far-red light treatment the PSI-LHCII complex was nearly undetectable, while it was present after blue light treatment, showing that state 1 and state 2 were successfully induced. Next, the stroma lamellae from state-1 and state-2 thylakoids were isolated [46]. The protein composition was analysed by SDS-PAGE followed by Coomassie staining, while Pro-Q diamond stain was used to analyse the degree of protein phosphorylation. The gel shows that LHCII is present in the stroma of state-1 plants (Fig. 3B). This LHCII is virtually unphosphorylated, in agreement with the absence of PSI-LHCII supercomplexes (Fig. 3A). Unphosphorylated LHCII is also found in the stroma lamellae of the ΔStn7 mutant, which lacks the LHCII kinase. LHCII gets phosphorylated upon transition to state 2 and the intensity of the LHCII Coomassie band increases with respect to the PSI Lhca antennas. The chlorophyll *a*/*b* ratio of 4.5 of the state-2 membranes is lower than that of the state-1 (chlorophyll *a*/b is 5.6) and ΔStn7 (chlorophyll *a*/b is 5.8) membranes, in agreement with a higher LHCII to PSI ratio and the association of LHCII with PSI (Fig. 3). There are also some PSII core proteins present in the stroma lamellae samples, which is expected because the stroma lamellae is the site where PSII core repair and assembly takes place [47]. Based on the protein composition it is not clear if the LHCII present in state-1 membranes functions as antenna of PSI and/or PSII.

3.3. LHCII transfers energy to PSI in state-1 and state-2 stroma lamellae

Low-temperature (77 K) fluorescence was used to investigate if LHCII in the stroma lamellae transfers energy to PSI and/or to PSII. The samples were measured before and after solubilisation with α-dodecyl maltoside (α-DM). Upon excitation of the intact membranes with 470 nm light the main fluorescence emission band has its maximum around 735 nm (Fig. 4). This is the emission maximum of PSI at 77 K and thus indicates that LHCII transfers excitation energy to PSI [15,21]. The small peak at 680–690 nm arises from LHCII and PSII complexes, which do not transfer energy to PSI. Upon solubilisation with α-DM LHCII disconnects from PSI and now shows fluorescence with a maximum at 680 nm [15]. The level of LHCII fluorescence relative to PSI is very similar for ΔStn7 and wild-type state-1 stroma lamellae, while it is about 1.7 times higher for state-2 membranes, as such confirming that more LHCII is present in state-2 membranes than in state-1 membranes.

3.4. Efficient energy transfer from LHCII to PSI in state-1 and state-2 stroma lamellae

Time-resolved fluorescence streak-camera measurements were used to investigate the energy transfer between LHCII and PSI in the stroma membranes. The fluorescence decay was measured after excitation with 400 nm light. The data is described by three decay-associated spectra as presented in Fig. 5. For the intact membranes (0% α-DM) the spectrum associated with a lifetime of 16–20 ps shows a typical excitation-energy transfer spectrum, with positive and negative amplitudes, and can be ascribed to energy transfer between the bulk chlorophylls of PSI and LHCII, and the red-shifted chlorophylls of PSI. The spectrum with a lifetime of 83–96 ps and a maximum at ~720 nm arises from the trapping of excitation energy by PSI. The 3rd spectrum, with a lifetime of 0.38–0.48 ns has PSII character and can be ascribed to a small amount of PSII complexes present in the stroma lamellae. Upon solubilisation with 0.5% α-DM the amplitude of the PSI trapping spectrum drops, indicating that the PSI antenna size decreases when LHCII dissociates. A new spectrum with a lifetime of ~3.7 ns and a maximum at 680 nm appears. This spectrum can be ascribed to LHCII in α-DM micelles, which indeed decays with this lifetime [48,49]. The 0.38–0.48 ns lifetime observed in the membranes is no longer resolved. The lifetime of these PSII complexes probably increased upon solubilisation and as such cannot be separated from the ~3.7 ns component. The shortest lifetime, which was ascribed to energy transfer in the intact membranes, now shows a mixture of excitation-energy trapping by PSI and energy transfer within PSI.

The area under the decay-associated spectra directly relates to the relative absorption cross section at the excitation wavelength of 400 nm (Table 1). If the 16–20 ps DAS is conservative, i.e. the positive part is equal to the negative part, this means that there is only excitation-energy transfer between the bulk chlorophylls *a* emitting around 680 nm and the red-shifted chlorophylls emitting around 720 nm. If the positive part is larger than the negative part, it may be that excitation-energy is also trapped by PSI. The net area of the 16–20 ps DAS was added to the 83–96 ps DAS to get the total PSI absorption cross section. The change in PSI antenna size upon disconnection of LHCII is smallest for the ΔStn7 and wild type state-1 stroma lamellae and largest for the wild-type state-2 membranes. The number of LHCII trimers transferring energy to PSI in the membrane can be calculated based on the relative absorption of LHCII and PSI and the change in PSI antenna size. Fig. 6 shows the absorption spectra of PSI and LHCII normalized to the

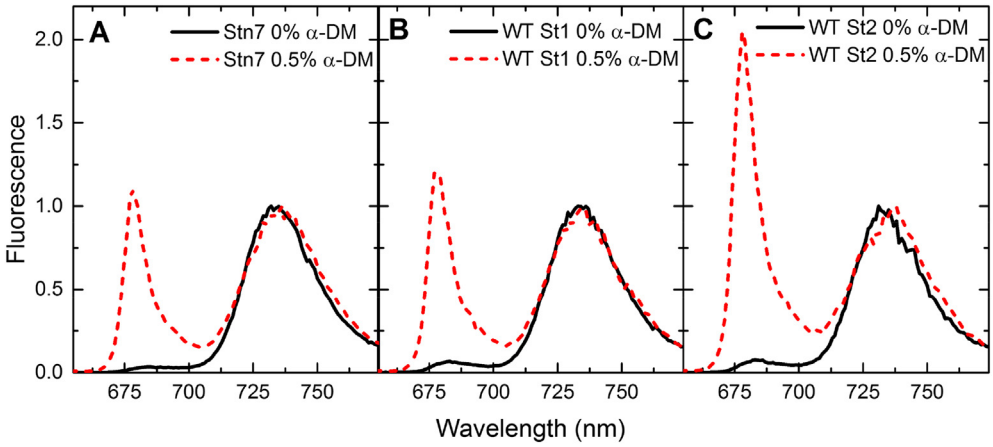

Fig. 4. 77 K steady-state fluorescence of intact and solubilised stroma lamellae. The steady state fluorescence of the stroma lamellae is recorded after excitation with 470 nm light. The membranes were either intact (0% α-DM) or solubilised (0.5% α-DM). LHCII which transfers energy to PSI in intact membranes becomes disconnected after solubilisation and emits at 680 nm. All spectra are normalized to the emission maximum of PSI at 733 nm.

number of chlorophylls they coordinate, e.g. 156 for PSI and 42 for LHCII. The absorption of PSI at 400 nm is four times larger than that of an LHCII trimer. The relative antenna size of PSI with LHCII attached in the stroma membranes versus PSI in solution (Table 1) can now be used to calculate how many LHCII trimers transfer energy to PSI in the stroma membranes. For instance, the 1.14 ± 0.04 times larger PSI antenna size in ΔStn7 stroma membranes compared to that of PSI in solution indicates that 0.14*4 = 0.5 ± 0.1 LHCII trimers are present per PSI in this sample. In state-1 membranes the calculation shows that 0.7 ± 0.1 LHCII trimers are present per PSI and in state-2 membranes 1.2 ± 0.1 LHCII trimer per PSI (Table 1).

The average PSI fluorescence lifetimes were used to calculate the energy trapping efficiency of PSI (φ_{PSI}) considering a loss rate of 0.4 /ns [49]. The trapping efficiency is close to unity for all samples, including the state-2 membranes where the PSI antenna size is enlarged by 1.2 LHCII trimers. This shows that LHCII is a very good PSI antenna.

Table 1
Number of LHCII trimers associated with PSI in stroma lamellae. The areas under the decay-associated spectra from Fig. 5 with lifetimes of ~20 ps and ~90 ps are related to the PSI-LHCII antenna size in intact membranes (0% α-DM) and to the PSI antenna size when LHCII is detached by membrane solubilisation (0.5% α-DM). The relative change in the PSI antenna size is used to calculate the number of LHCII trimers associated per PSI in the membrane. The average PSI-LHCII and PSI lifetimes $< \tau >$ are given. The average lifetimes are used to calculate the efficiency of energy trapping by PSI after excitation with 400 nm light ($\varphi_{PSI\ 400nm}$). The standard deviation (SD) values are based on two biological replicates.

Sample	Antenna size: PSI-LHCII/ PSI	LHCII trimers per PSI ± SD	$< \tau >$ PSI-LHCII and PSI ± SD	$\varphi_{PSI\ 400nm}$ ± SD
Stn7 0%	1.14 ± 0.04	0.5 ± 0.1	84 ± 1 ps	96.6 ± 0.1%
Stn7 0.5%			68 ± 0.3 ps	97.3 ± 0.01%
St1 0%	1.16 ± 0.03	0.7 ± 0.1	88 ± 4 ps	96.5 ± 0.1%
St1 0.5%			72 ± 5 ps	97.1 ± 0.2%
St2 0%	1.31 ± 0.04	1.2 ± 0.1	102 ± 7 ps	95.9 ± 0.3
St2 0.5%			76 ± 1 ps	97.0 ± 0.03

4. Discussion

4.1. LHCII is an efficient antenna of PSI under state-1 conditions

LHCII has classically been considered as an antenna of PSII which moves to PSI under special light conditions which over-excite PSII. We have already shown in the past that a considerable fraction of PSI is found in digitonin stable PSI-LHCII supercomplexes under normal grow light conditions [19]. In these complexes LHCII is phosphorylated and associates with PSI at the PsaH/L/O side [12,15,18]. However, recent reports have indicated that LHCII also transfers energy to PSI in state-1, e.g. when PSI is over-excited and LHCII is not phosphorylated [16,22,24]. Using time-resolved fluorescence measurements we have now determined that 0.5–0.7 ± 0.1 LHCII trimers are present per PSI in wild-type state-1 and Stn7 stroma membranes, in good agreement with the value of 0.8 reported by Bressan et al. for state-1 stroma membranes based on biochemical quantification [24] and with the presence of LHCII in state-1 stroma membranes [54]. Our data shows that this digitonin sensitive unphosphorylated LHCII transfers its energy to PSI with high efficiency.

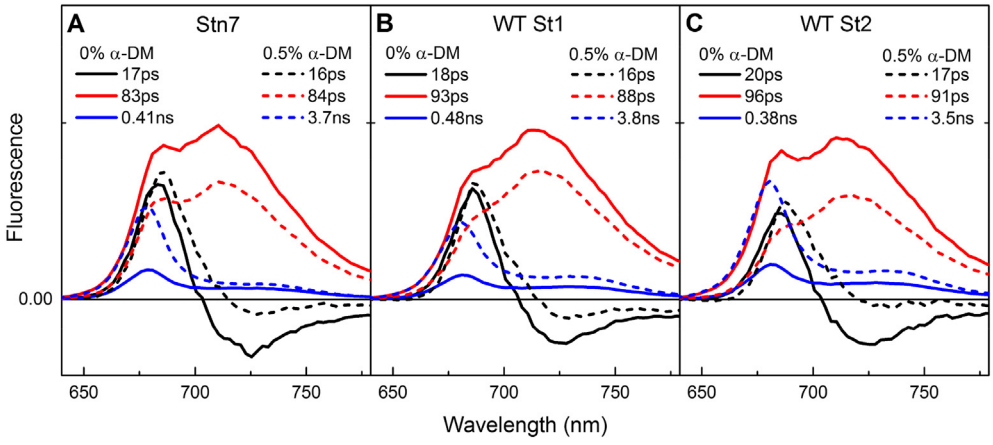

Fig. 5. Fluorescence decay of stroma lamellae. Decay-associated spectra of ΔStn7 and wild-type state-1 (WT St1) and state-2 (WT St2) stroma membranes after 400 nm excitation. The membranes were either intact (0% α-DM) or solubilised (0.5% α-DM). The solubilised samples were not centrifuged before measuring, meaning that the protein composition is exactly the same for the solubilised and unsolubilised samples. The total area under the spectra is normalized to 1.

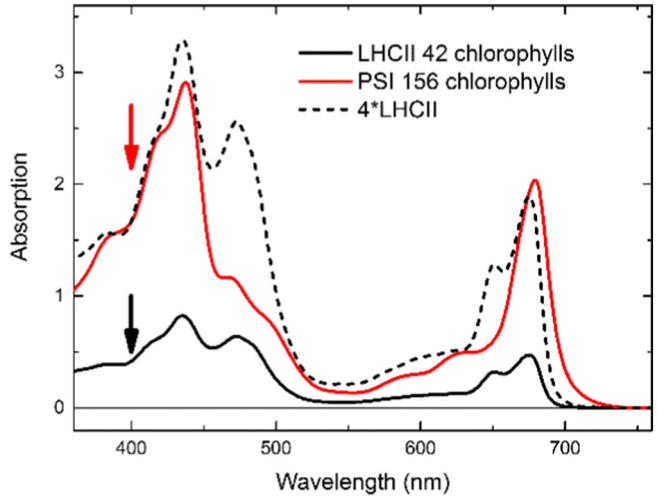

Fig. 6. Absorption of PSI and LHCII normalized to 156 [50,51] and 42 [52] chlorophylls, respectively, considering a chlorophyll *a*/b ratio of 8.5 for PSI and 1.3 for LHCII as in [2] and a 0.7 times weaker oscillator strength of chlorophyll *b* in the Q_y region from 630 to 750 nm [53]. The absorption at 400 nm is indicated with an arrow.

4.2. How much does the PSI antenna size change during state transitions?

Time-resolved fluorescence on leaves does not only show the change in antenna size of PSII upon state transitions, but also that of PSI. The change in PSI antenna size or qT_{PSI} can be used to calculate how much LHCII moves from PSII in state-1 to PSI in state-2 in intact leaves. The amount of PSI fluorescence is directly related to its antenna size. In state-1 the antenna size of PSI in the stroma membranes is enlarged by 0.7 ± 0.1 LHCII trimers (see Results Section 3.4). The absorption of PSI + 0.7 LHCII at 400 nm can be calculated based on the normalized absorption spectra of PSI and LHCII in Fig. 6. From the qT_{PSI} value of 0.11 ± 0.01 it follows that the PSI antenna is increased with 0.58 ± 0.06 LHCII trimers in state-2 as compared to state-1 (see Materials and Methods for details). At 483 nm excitation qT_{PSI} was 0.19 ± 0.01, and based on the absorption cross sections of PSI and LHCII at this wavelength the enlargement of PSI in state-2 is 0.55 ± 0.04 LHCII trimers. Thus the two results based on excitation at 400 nm and 483 nm are consistent. The total number of LHCII trimers per PSI in state-2 is ~1.3 according to these calculations, close to the measured value of 1.2 ± 0.1 LHCII trimers found in the stroma membranes. These calculations are based on the PSI antenna size in stroma lamellae in state-1, but what if the average number of LHCII trimers is different in the entire thylakoids? In the extreme case that there would be no LHCII associated with PSI in state-1, the calculations indicate that 0.49 ± 0.05 (400 nm excitation) or 0.38 ± 0.03 (483 nm excitation) LHCII trimers associate with PSI upon state-1 to state-2 transition. If instead already 1 LHCII trimer would be present per PSI in state-1, then the increase would be 0.62 ± 0.05 LHCII (based on both excitation wavelengths) upon transition to state-2. It is as such safe to assume that the PSI antenna size increases by 0.5 ± 0.1 LHCII trimers upon transition to state-2. Indeed, this is close to the fraction of digitonin stable PSI-LHCII supercomplexes observed in state-2 membranes [17,19,22]. It can thus be suggested that the enlargement of the PSI antenna size in state-2 is largely caused by the association of LHCII-P at the PsaH/L/O side of PSI, although a fraction of LHCII-P might associate with PSI at other positions. Association of LHCII at other positions, such as the Lhca antennae [22,23], could explain why ΔPsaH/L mutant plants still show 20–30% state transitions as compared to the wild-type level [13,22].

Is the change in PSI antenna size consistent with that of PSII? In this study we did not measure the PSII antenna size. However, we have shown previously that PSII of *A. thaliana* plants grown under moderate light conditions is mainly composed of a dimeric core, 2 S-trimers and 2 M-trimers, called $C_2S_2M_2$ [6,55,56]. Also it was shown that the mobile LHCII trimers involved in state transitions are not part of the $C_2S_2M_2$ supercomplex [6,15]. Assuming that the PSI/PSII core ratio is close to unity [44], this means that the PSII antenna size should be enlarged by at least 0.5 ± 0.1 "extra" LHCII trimers in State-1. Based on the qT_{PSII} values (0.12 at 400 nm and 0.14 at 483 nm) and on the absorption spectra of LHCII (Fig. 4) and of $C_2S_2M_2$ [25] (coordinating 157 chlorophylls per monomer [57]) it follows that the PSII antenna size decreases with 0.48–0.56 LHCII trimers per PSII core upon state-1 to state-2 transition. This value is consistent with the calculated increase of the PSI antenna size of 0.5 ± 0.1 LHCII trimers per PSI.

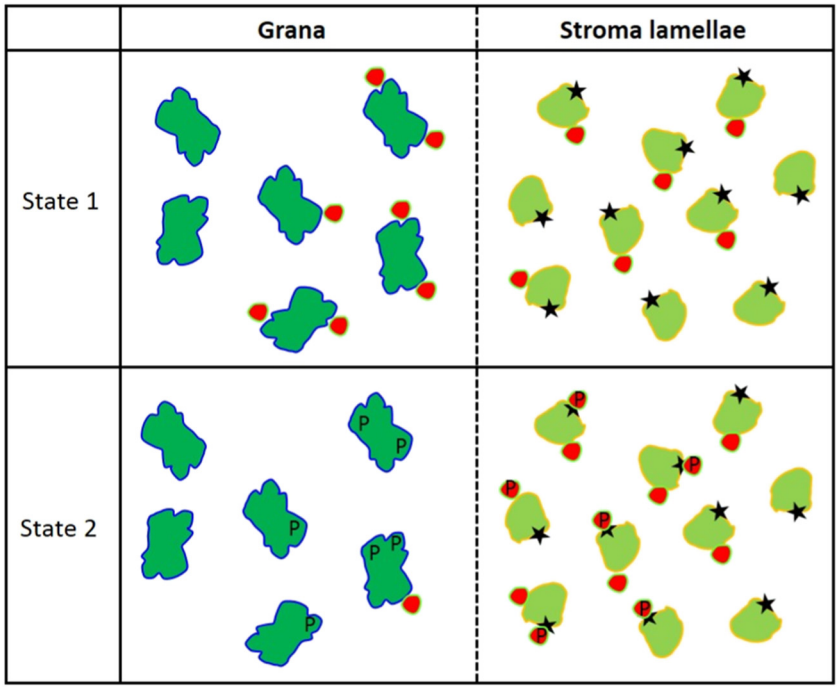

Fig. 7. Model of state transitions in *A. thaliana* plants. $C_2S_2M_2$ PSII complexes (dark green) are located in the grana membranes and PSI complexes (light green) in the stroma lamellae. In state-1 conditions unphosphorylated "extra" LHCII trimers (red) enlarge the antenna cross section of both PSI and PSII. Upon over-excitation of PSII the "extra" LHCII trimers in the grana become phosphorylated (P) by Stn7 and move to the stroma membrane to associate with PSI at the PsaH/L/O side (black star). Some P-LHCII might also associate with PSI at another position. (For interpretation of the references to colour in this figure legend, the reader is referred to the web version of this article.)

4.3. Updated model for state transitions

Fig. 7 summarises our present view of state transitions in *A. thaliana* plants grown under normal light conditions. In state-1 $C_2S_2M_2$ PSII supercomplexes are located in the grana membranes [55,58]. The absorption cross section is enlarged by "extra" LHCII trimers of which the position with respect to the PSII supercomplex is unclear [6,15]. In the stroma membranes about 0.6–0.7 unphosphorylated LHCII trimers per PSI enlarge the antenna cross section of PSI. The location of these LHCIIs is not known, although it has been suggested that they interact with the Lhca antennae [22,23]. On the other hand Bressan et al. found multiple LHCII trimers per PSI in stroma membranes from ΔLhca mutant plants, which suggests that LHCII can also interact with the PSI core [24]. The interaction between LHCII and PSI might also be unspecific, as LHCII complexes seem to cluster whenever they are in a membrane [59]. Upon the transition to state-2 conditions the "extra" LHCII trimers composed of $Lhcb1_2Lhcb2_1$ isoforms get phosphorylated at Lhcb2 [9,10] and associate with PSI at the PsaH/L/O side [12,15,18]. Some LHCII-P might also associate with PSI at other positions, which could explain the residual state transitions in ΔPsaH/L plants [13]. In total an average of 1.2–1.3 LHCII trimers transfer energy to PSI in state-2. About one out of three LHCII trimers from the $C_2S_2M_2$ supercomplexes also gets phosphorylated [9]. The phosphorylation level of LHCII is lower in the grana core compared to the periphery of the grana [9]. Phosphorylation of the S- and M-trimers might facilitate the dissociation of the "extra" LHCII trimers from the PSII supercomplex [55,60].

4.4. Open questions

The observation that unphosphorylated LHCII is present in state-1 stroma membranes opens up new questions. Do these LHCII trimers have specific post-translational modifications directing them to the stroma lamellae? At which side do they associate with PSI? How does this LHCII affect the wavelength dependence of the excitation balance between PSI and PSII [2]? If plants grow under low light the LHCII content increases, and it has been assumed that this LHCII enlarges the antenna cross section of PSII and only that of PSI by the association of LHCII-P in state-2 conditions [19]. However, in light of the data presented here it can be hypothesized that the PSI antenna size is already larger in low light grown plants by elevated LHCII levels in the stroma membranes. Further research is required to answer these questions.

Transparency document

The Transparency document associated with this article can be found, in online version.

Funding

This work was supported by a Veni grant (016.161.038; E.W.) from The Netherlands Organisation for Scientific Research (NWO), Earth and Life Sciences (ALW).

References

[1] R.E. Blankenship, Molecular Mechanisms of Photosynthesis, Wiley Blackwell, 2014.
[2] S.W. Hogewoning, E. Wientjes, P. Douwstra, G. Trouwborst, W. van Ieperen, R. Croce, J. Harbinson, Photosynthetic quantum yield dynamics: from photosystems to leaves, Plant Cell 24 (2012) 1921–1935.
[3] J.F. Allen, State transitions - a question of balance, Science 299 (2003) 1530–1532.
[4] J.D. Rochaix, Regulation and dynamics of the light-harvesting system, Annu. Rev. Plant Biol. 65 (2014) 287–309.
[5] S. Bellafiore, F. Bameche, G. Peltier, J.D. Rochaix, State transitions and light adaptation require chloroplast thylakoid protein kinase STN7, Nature 433 (2005) 892–895.
[6] E. Wientjes, H. van Amerongen, R. Croce, Quantum yield of charge separation in photosystem II: functional effect of changes in the antenna size upon light acclimation, J. Phys. Chem. B (2013), https://doi.org/10.1021/jp401663w.
[7] M. Pribil, P. Pesaresi, A. Hertle, R. Barbato, D. Leister, Role of plastid protein phosphatase TAP38 in LHCII dephosphorylation and thylakoid electron flow, PLoS Biol. 8 (2010).
[8] A. Shapiguzov, B. Ingelsson, I. Samol, C. Andres, F. Kessler, J.D. Rochaix, A.V. Vener, M. Goldschmidt-Clermont, The PPH1 phosphatase is specifically involved in LHCII dephosphorylation and state transitions in Arabidopsis, Proc. Natl. Acad. Sci. U. S. A. 107 (2010) 4782–4787.
[9] A. Crepin, S. Caffarri, The specific localizations of phosphorylated Lhcb1 and Lhcb2 isoforms reveal the role of Lhcb2 in the formation of the PSI-LHCII supercomplex in Arabidopsis during state transitions, BBA-Bioenergetics 1847 (2015) 1539–1548.
[10] P. Longoni, D. Douchi, F. Cariti, G. Fucile, M. Goldschmidt-Clermont, Phosphorylation of the light-harvesting complex II isoform Lhcb2 is central to state transitions, Plant Physiol. 169 (2015) 2874–2883.
[11] M. Pietrzykowska, M. Suorsa, D.A. Semchonok, M. Tikkanen, E.J. Boekema, E.M. Aro, S. Jansson, The light-harvesting chlorophyll a/b binding proteins Lhcb1 and Lhcb2 play complementary roles during state transitions in Arabidopsis, Plant Cell 26 (2014) 3646–3660.
[12] X.W. Pan, J. Ma, X.D. Su, P. Cao, W.R. Chang, Z.F. Liu, X.Z. Zhang, M. Li, Structure of the maize photosystem I supercomplex with light-harvesting complexes I and II, Science 360 (2018) 1109–1112.
[13] C. Lunde, P.E. Jensen, A. Haldrup, J. Knoetzel, H.V. Scheller, The PSI-H subunit of photosystem I is essential for state transitions in plant photosynthesis, Nature 408 (2000) 613–615.
[14] S.P. Zhang, H.V. Scheller, Light-harvesting complex II binds to several small subunits of Photosystem I, J. Biol. Chem. 279 (2004) 3180–3187.
[15] P. Galka, S. Santabarbara, T.T. Khuong, H. Degand, P. Morsomme, R.C. Jennings, E.J. Boekema, S. Caffarri, Functional analyses of the plant Photosystem I-Light-Harvesting Complex II supercomplex reveal that light-harvesting complex II loosely bound to Photosystem II is a very efficient antenna for Photosystem I in state II, Plant Cell 24 (2012) 2963–2978.
[16] M. Grieco, M. Suorsa, A. Jajoo, M. Tikkanen, E.M. Aro, Light-harvesting II antenna trimers connect energetically the entire photosynthetic machinery - including both photosystems II and I, Biochim. Biophys. Acta 1847 (2015) 607–619.
[17] S. Jarvi, M. Suorsa, V. Paakkarinen, E.M. Aro, Optimized native gel systems for separation of thylakoid protein complexes: novel super- and mega-complexes, Biochem. J. 439 (2011) 207–214.
[18] R. Kouril, A. Zygadlo, A.A. Arteni, C.D. de Wit, J.P. Dekker, P.E. Jensen, H.V. Scheller, E.J. Boekema, Structural characterization of a complex of photosystem I and light-harvesting complex II of *Arabidopsis thaliana*, Biochemistry-Us 44 (2005) 10935–10940.
[19] E. Wientjes, H. van Amerongen, R. Croce, LHCII is an antenna of both photosystems after long-term acclimation, BBA-Bioenergetics 1827 (2013) 420–426.
[20] A.J. Bell, L.K. Frankel, T.M. Bricker, High yield non-detergent isolation of Photosystem I-lightharvesting chlorophyll II membranes from spinach thylakoids implications for the organization of the PS I antennae in higher plants, J. Biol. Chem. 290 (2015) 18429–18437.
[21] I. Bos, K.M. Bland, L. Tian, R. Croce, L.K. Frankel, H. van Amerongen, T.M. Bricker, E. Wientjes, Multiple LHCII antennae can transfer energy efficiently to a single Photosystem I, Biochim. Biophys. Acta 1858 (2017) 371–378.
[22] S.L. Benson, P. Maheswaran, M.A. Ware, C.N. Hunter, P. Horton, S. Jansson, A.V. Ruban, M.P. Johnson, An intact light harvesting complex I antenna system is required for complete state transitions in Arabidopsis, Nat. Plants 15176 (2015).
[23] K.N. Yadav, D.A. Semchonok, L. Nosek, R. Kouril, G. Fucile, E.J. Boekema, L.A. Eichacker, Supercomplexes of plant photosystem I with cytochrome b_6f, light-harvesting complex II and NDH, Biochim. Biophys. Acta 1858 (2017) 12–20.
[24] M. Bressan, R. Bassi, L. Dall'Osto, Loss of LHCI system affects LHCII re-distribution between thylakoid domains upon state transitions, Photosynth. Res. 135 (2018) 251–261.
[25] S. Caffarri, R. Kouřil, S. Kereïche, E.J. Boekema, R. Croce, Functional architecture of higher plant photosystem II supercomplexes, EMBO J. 28 (2009) 3052–3063.
[26] R. Fristedt, A. Willig, P. Granath, M. Crevecoeur, J.D. Rochaix, A.V. Vener, Phosphorylation of photosystem II controls functional macroscopic folding of photosynthetic membranes in Arabidopsis, Plant Cell 21 (2009) 3950–3964.
[27] R. Croce, G. Canino, F. Ros, R. Bassi, Chromophore organization in the higher-plant Photosystem II antenna protein CP26, Biochemistry-Us 41 (2002) 7334–7343.
[28] M. Ballottari, C. Govoni, S. Caffarri, T. Morosinotto, Stoichiometry of LHCI antenna polypeptides and characterization of gap and linker pigments in higher plants Photosystem I, Eur. J. Biochem. 271 (2004) 4659–4665.
[29] B. van Oort, S. Murali, E. Wientjes, R.B.M. Koehorst, R.B. Spruijt, A. van Hoek, R. Croce, H. van Amerongen, Ultrafast resonance energy transfer from a site-specifically attached fluorescent chromophore reveals the folding of the N-terminal domain of CP29, Chem. Phys. 357 (2009) 113–119.
[30] A.R. Holzwarth, Y. Miloslavina, M. Nilkens, P. Jahns, Identification of two quenching sites active in the regulation of photosynthetic light-harvesting studied by time-resolved fluorescence, Chem. Phys. Lett. 483 (2009) 262–267.
[31] S. Farooq, J. Chmeliov, E. Wientjes, R. Koehorst, A. Bader, L. Valkunas, G. Trinkunas, H. van Amerongen, Dynamic feedback of the photosystem II reaction centre on photoprotection in plants, Nat. Plants 4 (2018) 225–231.
[32] K.M. Mullen, I.H.M. van Stokkum, TIMP: an R package for modeling multi-way spectroscopic measurements, J. Stat. Softw. 18 (2007) 1–46.
[33] J.J. Snellenburg, S.P. Laptenok, R. Seger, K.M. Mullen, I.H.M. van Stokkum, Glotaran: a Java-based graphical user interface for the R package TIMP, J. Stat. Softw. 49 (2012) 1–22.
[34] E. Wientjes, J. Philippi, J.W. Borst, H. van Amerongen, Imaging the Photosystem I/Photosystem II chlorophyll ratio inside the leaf, Biochim. Biophys. Acta 1858

(2017) 259–265.
[35] E. Kim, T.K. Ahn, S. Kumazaki, Changes in antenna sizes of photosystems during state transitions in granal and stroma-exposed thylakoid membrane of intact chloroplasts in Arabidopsis mesophyll protoplasts, Plant Cell Physiol. 56 (2015) 759–768.
[36] R. Croce, D. Dorra, A.R. Holzwarth, R.C. Jennings, Fluorescence decay and spectral evolution in intact photosystem I of higher plants, Biochemistry-Us 39 (2000) 6341–6348.
[37] E. Engelmann, G. Zucchelli, A.P. Casazza, D. Brogioli, F.M. Garlaschi, R.C. Jennings, Influence of the photosystem I - light harvesting complex I antenna domains on fluorescence decay, Biochemistry-Us 45 (2006) 6947–6955.
[38] J.A. Ihalainen, F. Klimmek, U. Ganeteg, I.H.M. van Stokkum, R. van Grondelle, S. Jansson, J.P. Dekker, Excitation energy trapping in photosystem I complexes depleted in Lhca1 and Lhca4, FEBS Lett. 579 (2005) 4787–4791.
[39] C. Slavov, M. Ballottari, T. Morosinotto, R. Bassi, A.R. Holzwarth, Trap-limited charge separation kinetics in higher plant photosystem I complexes, Biophys. J. 94 (2008) 3601–3612.
[40] E. Wientjes, I.H.M. van Stokkum, H. van Amerongen, R. Croce, The role of the individual Lhcas in photosystem I excitation energy trapping, Biophys. J. 101 (2011) 745–754.
[41] E. Wientjes, R. Croce, PMS: photosystem I electron donor or fluorescence quencher, Photosynth. Res. 111 (2012) 185–191.
[42] R. Croce, A. Chojnicka, T. Morosinotto, J.A. Ihalainen, F. van Mourik, J.P. Dekker, R. Bassi, R. van Grondelle, The low-energy forms of photosystem I light-harvesting complexes: spectroscopic properties and pigment-pigment interaction characteristics, Biophys. J. 93 (2007) 2418–2428.
[43] A.V. Ruban, M.P. Johnson, Dynamics of higher plant photosystem cross-section associated with state transitions, Photosynth. Res. 99 (2009) 173–183.
[44] R. Danielsson, P.A. Albertsson, F. Mamedov, S. Styring, Quantification of photosystem I and II in different parts of the thylakoid membrane from spinach, BBA-Bioenergetics 1608 (2004) 53–61.
[45] S. Caffarri, R. Croce, L. Cattivelli, R. Bassi, A look within LHCII: differential analysis of the Lhcbl-3 complexes building the major trimeric antenna complex of higher-plant photosynthesis, Biochemistry-Us 43 (2004) 9467–9476.
[46] R. Barbato, E. Bergo, I. Szabo, F. Dalla Vecchia, G.M. Giacometti, Ultraviolet B exposure of whole leaves of barley affects structure and functional organization of photosystem II, J. Biol. Chem. 275 (2000) 10976–10982.
[47] E.M. Aro, I. Virgin, B. Andersson, Photoinhibition of Photosystem-2 - inactivation, protein damage and turnover, Biochim. Biophys. Acta 1143 (1993) 113–134.
[48] M.A. Palacios, F.L. de Weerd, J.A. Ihalainen, R. van Grondelle, H. van Amerongen, Superradiance and exciton (de)localization in light-harvesting complex II from green plants? J. Phys. Chem. B 106 (2002) 5782–5787.
[49] E. Wientjes, I.H. van Stokkum, H. van Amerongen, R. Croce, Excitation-energy transfer dynamics of higher plant photosystem I light-harvesting complexes, Biophys. J. 100 (2011) 1372–1380.
[50] Y. Mazor, A. Borovikova, N. Nelson, The structure of plant photosystem I supercomplex at 2.8 angstrom resolution, Elife 4 (2015).
[51] X.C. Qin, M. Suga, T.Y. Kuang, J.R. Shen, Structural basis for energy transfer pathways in the plant PSI-LHCI supercomplex, Science 348 (2015) 989–995.
[52] Z. Liu, H. Yan, K. Wang, T. Kuang, J. Zhang, L. Gui, X. An, W. Chang, Crystal structure of spinach major light-harvesting complex at 2.72 A resolution, Nature 428 (2004) 287–292.
[53] K. Sauer, J.R.L. Smith, A.J. Schultz, Dimerization of chlorophyll a chlorophyll b and bacteriochlorophyll in solution, J. Am. Chem. Soc. 88 (1966) 2681.
[54] W.H.J. Wood, C. MacGregor-Chatwin, S.F.H. Barnett, G.E. Mayneord, X. Huang, J.K. Hobbs, C.N. Hunter, M.P. Johnson, Dynamic thylakoid stacking regulates the balance between linear and cyclic photosynthetic electron transfer, Nat. Plants 4 (2018) 116–127.
[55] E. Wientjes, B. Drop, R. Kouril, E.J. Boekema, R. Croce, During state 1 to state 2 transition in Arabidopsis thaliana the Photosystem II supercomplex gets phosphorylated but does not disassemble, J. Biol. Chem. 288 (2013) 32821–32826.
[56] J.P. Dekker, E.J. Boekema, Supramolecular organization of thylakoid membrane proteins in green plants, BBA-Bioenergetics 1706 (2005) 12–39.
[57] X.D. Su, J. Ma, X.P. Wei, P. Cao, D.J. Zhu, W.R. Chang, Z.F. Liu, X.Z. Zhang, M. Li, Structure and assembly mechanism of plant C2S2M2-type PSII-LHCII supercomplex, Science 357 (2017) 816.
[58] R. Kouril, E. Wientjes, J. Bultema, R. Croce, E. Boekema, High-light vs. low-light: effect of light acclimation on photosystem II composition and organization in Arabidopsis thaliana, Bba-Bioenergetics 1827 (2013) 411–419.
[59] A. Natali, J.M. Gruber, L. Dietzel, M.C.A. Stuart, R. van Grondelle, R. Croce, Light-harvesting complexes (LHCs) cluster spontaneously in membrane environment leading to shortening of their excited state lifetimes, J. Biol. Chem. 291 (2016) 16730–16739.
[60] S. Puthiyaveetil, B. van Oort, H. Kirchhoff, Surface charge dynamics in photosynthetic membranes and the structural consequences, Nat. Plants. 3 (2017).